

Original Article

DOI 10.1007/s12206-023-0304-1

Keywords:

- Ball screw
- Overturning moment
- Nonuniform load distribution
- Distribution fluctuation

Correspondence to:

Yongjiang Chen
545541301@qq.com

Citation:

Chen, Y., Zhao, J., Yuan, C., Sun, J. (2023). Analysis of contact characteristics of ball screws under the combined loads considering non-uniform load distribution. *Journal of Mechanical Science and Technology* 37 (4) (2023) 1613~1621. <http://doi.org/10.1007/s12206-023-0304-1>

Received June 19th, 2022

Revised September 15th, 2022

Accepted December 17th, 2022

† Recommended by Editor
No-cheol Park

Analysis of contact characteristics of ball screws under the combined loads considering non-uniform load distribution

Yongjiang Chen¹, Jianghai Zhao², Chuangfan Yuan² and Jingkai Sun²

¹School of Aerospace and Mechanical Engineering, Changzhou Institute of Technology, Changzhou 213002, China, ²Institute of Advanced Manufacturing Technology, Chinese Academy of Sciences, Changzhou 213164, China

Abstract An analysis model of the contact characteristics of the double-nut preloaded ball screw which can consider the combined action of the axial load and the overturning moment is established, the model can consider non-uniform load distribution, and the validity of the model is verified by experiments. Based on this model, the influence of the combined action of axial load and overturning moment on the average value and distribution fluctuation value of the contact angle of the ball screw, the number of unloaded balls, the distribution fluctuation value of the contact load, and the static contact stiffness and other contact parameters are systematically analyzed, and get the following conclusions: The contact parameters of the ball screw are mainly affected by the axial load and the contact state between the ball and the raceway. The gradually increasing axial load basically reduces the influence of the overturning moment on the contact parameters of the ball screw. There is a critical value of the load in the axial direction within the range of the action value of the preload load. Only when the critical value is above the critical value, the contact parameters will change regularly with the changes in the axial stiffness and overturning moment. However, different critical values for the regular variation of contact parameters with axial load and overturning moment vary.

1. Introduction

Ball screws have become one of the most widely used rolling functional components for positioning and transmission due to their high rigidity, high load-bearing capacity, and high precision [1, 2]. The contact angle and contact load between the ball and the raceway in the ball screw are the main parameters that affect the motion behavior and mechanical properties of the ball screw, and their values are also the basis for solving the static contact stiffness. The static contact stiffness is an important performance index of the ball screw, which can not only reflect its bearing capacity but also directly affect the positioning accuracy of the machine tool [3-5]. In the commonly used application scenarios of ball screws, the ball screw is mainly affected by the axial load. However, when the ball screw is installed with one end thrust and the other free, the screw is subjected to rotary centrifugal force and gravity during horizontal installation. As a result, the ball screw is also subjected to an overturning moment [6, 7]. Therefore, an analysis model of the contact characteristics of the ball screw that can consider the combined action of the axial load and the overturning moment is established, and the average value and distribution fluctuation of the contact angle of the ball screw caused by the combined load, the number of unloaded balls and the distribution fluctuation of the contact load are studied. The influence of contact parameters such as value and static contact stiffness is of great significance.

The basis for the establishment of the contact characteristic analysis model of the ball screw is the establishment of its internal load distribution model. Many scholars have researched the internal load distribution of the ball screw. Bertolaso et al. [8] tried to obtain the internal load distribution of the ball screw through two measurement techniques of photoelastometer and marker tracking. However, the experimental measurement method is difficult to implement, the

data obtained is limited, and the internal load distribution of the ball screw cannot be fully analyzed, so the model-based analysis method of the internal load of the ball screw is adopted by most scholars. Lin et al. [9] established a low-order static load distribution ball screw hybrid finite element model by using the finite element method and analyzed the influence of geometric errors and ball diameter changes on the internal load distribution. Luca et al. [10] established a high-order ball screw finite element model and analyzed the influence of many factors on the internal load of the ball screw. The results show that the force analysis object and the direction of the load have a great influence (the overturning direction is not considered). However, the establishment of the contact model between the ball and the raceway has always been a difficult problem in the establishment of the finite element model of the ball screw, and the above studies all simplify the contact part. Zhao et al. [11] and Liu et al. [12] took the lead screw as the analysis object and based on the coordinated deformation relationship between the axial deformation of the lead screw and the normal contact of the ball, the static equilibrium of the two-degree-of-freedom and three-degree-of-freedom ball screw was established respectively. According to the equation system, the internal load distribution of the ball screw is analyzed.

However, the modeling method of the ball screw contact characteristic analysis model considering non-uniform load distribution is less studied. Chen et al. [13] took the screw raceway as the analysis object and only considering the force and torque of a circle of balls on the screw raceway, a three-degree-of-freedom ball screw static equilibrium equation system is established. Liu et al. [14] analyzed the effects of geometric error, preload load, and axial external load on the static contact stiffness of the ball screw based on the two-degree-of-freedom ball screw static equilibrium equations.

To sum up, most of the existing studies only consider the influence of the axial load on the contact characteristics of the ball screw, when the ball screw is installed with one end thrust and the other free, its contact characteristics are also affected by overturning moments. In addition, most of the existing contact characteristic analysis models consider less degree of freedom of raceway deformation and do not conduct an in-depth analysis of the influence of non-uniform load distribution on contact characteristics. Therefore, this paper proposes a ball screw contact characteristic analysis model that can consider the combined effect of non-uniform load distribution, axial load, and overturning moment, in-depth analysis of the influence of the combined action of axial load and overturning moment on the average value and distribution fluctuation value of the ball screw contact angle, the number of unloaded balls, the distribution fluctuation value of the contact load, and the static contact stiffness and other contact parameters.

2. Modeling

Under the combined action of axial load and overturning moment, the basis for the analysis of the contact characteris-

tics of the ball screw is the solution of contact parameters such as contact angle, contact load static contact stiffness, etc., and the key to obtaining the contact parameters is the construction of the contact deformation coordination relationship between the ball and the raceway. In practical applications, the transmission mode of the ball screw is often used for the rotation of the screw and the linear motion of the nut. According to this, it can be assumed that the nut raceway is fixed, the screw raceway is selected as the analysis object, and establish an absolute coordinate system (O, x, y, z) at the geometric center of the screw raceway [15]. The construction of the contact deformation coordination relationship between the ball and the raceway can be based on the Hertzian contact theory, the geometric relationship between the three points of the nut raceway curvature center, the screw raceway curvature center, and the ball center is obtained by analyzing the two states of the screw raceway with or without load. To this end, a moving coordinate system (O', x', y', z') is established to describe the motion of the ball center on the cylindrical helical trajectory, and a local coordinate system $(O'', y'', z'', \Theta'')$ is established to describe the relationship between the center of curvature and the center of the ball. When the double nut washer preloaded ball screw is installed with one end fixed and one end supported as shown in Fig. 1, a moment will be generated around the X-axis, which is the overturning moment. The effect of the overturning moment will cause a certain deviation between the axis of the screw and the axis of the nut, as shown in Fig. 1. The inclination direction of the lead screw is positive, that is, the direction of counterclockwise rotation around the x-axis based on the right-hand principle.

When only preloaded, there are two states of contact between the ball and the raceway in the double nut washer preloaded ball screw, as shown in Fig. 2. The two nuts are called the straight nut and flange nut, respectively. The action value and direction of the axial load will have a direct impact on the state of contact between the ball and the raceway when the screw raceway is subjected to an axial load in the positive direction of the shaft: When the axial load is less than the preload load, the two contact states between the ball and the

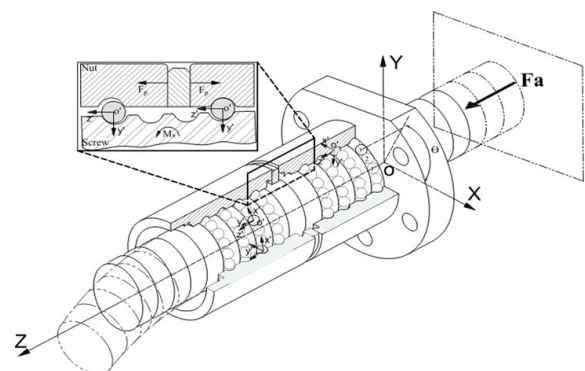


Fig. 1. Structure diagram of ball screw under the combined action of axial load and overturning moment.

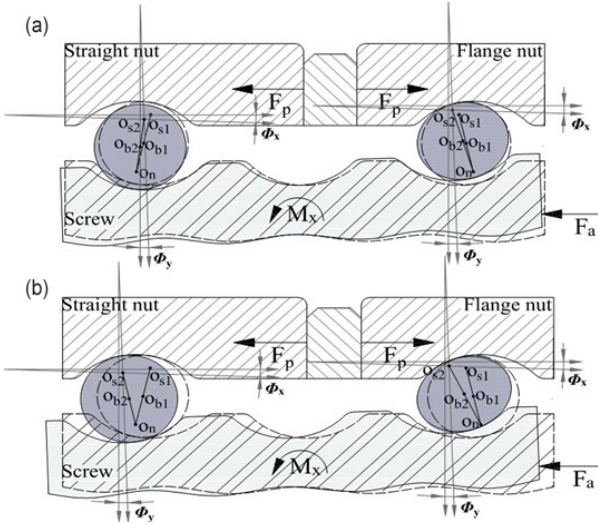


Fig. 2. Contact state between balls and raceways: (a) axial load is less than preload; (b) axial load is greater than preload.

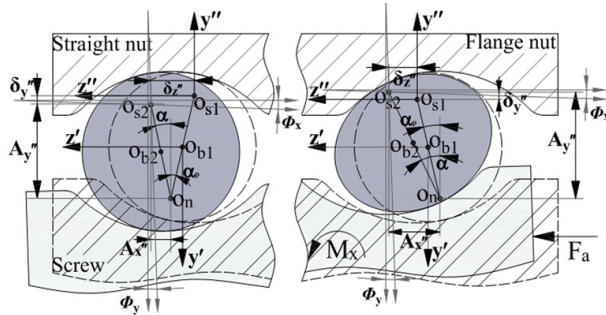


Fig. 3. The relationship between the position of the center of curvature of the screw and nut raceway.

raceway remain unchanged, as shown in Fig. 2(a); When the axial load is greater than the preload load, the contact state between the balls in the straight nut and the screw raceway will change, so at this time, the contact state of the balls in the two nuts and the raceway is the same, as shown in Fig. 2(b).

Since the static ball screw does not need to consider the effect of centrifugal force, it can be seen from the relationship between the center of curvature of the raceway and the center of the ball as shown in Fig. 3, the center of curvature of the nut raceway, the ball center of the ball and the center of curvature of the screw raceway are all located on a straight line in both states with and without load: Only under the action of preloading load, the angle between the connecting line between the center of curvature of the nut raceway and the center of curvature of the screw raceway and the shaft is the initial contact angle of α_p ; Under the combined action of the axial load and the overturning moment, the center of curvature of the screw raceway will move from O_{s1} to O_{s2} , and move $\delta_{z''}$ and $\delta_{y''}$, respectively along the z'' and y'' axis directions, and the contact angle changes from α_p to α_j , the calculation formula of α_j is:

$$\alpha_j = \arctan\left(\frac{A_{zj}}{A_{yj}}\right) = \arctan\left(\frac{BD \sin \alpha_p + \delta_{z''j}}{BD \cos \alpha_p + \delta_{y''j}}\right) \quad (1)$$

where BD is the distance between the nut raceway and the center of curvature of the screw raceway before contact deformation; A_{yj} and A_{zj} are the axis y'' and z'' on-axis components of the distance (O_{NS2}) between the nut raceway curvature center and the deformed screw raceway center of curvature, respectively, where the subscripts j are the numerical numbers of the phase angles where the balls are located at different phase angles, $\delta_{y''j}$ and $\delta_{z''j}$ the expressions of as shown in Eq. (2).

$$\begin{aligned} \delta_{y''j} &= -C_{\theta_j} u_{xj} - S_{\theta_j} u_{yj} + S_{\theta_j} \sigma_{3j} \phi_{xj} - C_{\theta_j} \sigma_{3j} \phi_{yj} \\ \delta_{z''j} &= S_a S_{\theta_j} u_{xj} - C_{\theta_j} S_a u_{yj} + C_a u_{zj} + (C_a \sigma_{2j} + S_a C_{\theta_j} \sigma_{3j}) \phi_{xj} \\ &\quad + (S_a S_{\theta_j} \sigma_{3j} - C_a \sigma_{1j}) \phi_{yj} \end{aligned} \quad (2)$$

where θ_j is the ball phase angle, S_{θ_j} and C_{θ_j} are the simplified expressions of $\sin \theta_j$ and $\cos \theta_j$, respectively; a is the helix angle, S_a and C_a are the simplified expressions of $\sin a$ and $\cos a$ respectively; u_{xj} , u_{yj} and u_{zj} are the displacement deformations in the three directions of x , y and z respectively, ϕ_{xj} and ϕ_{yj} are the angular deformations around x and y respectively; The expressions of σ_{1j} , σ_{2j} and σ_{3j} are shown in Eq. (3).

$$\begin{aligned} \sigma_{1j} &= r_0 C_{\theta_j} + C_{\theta_j} C_a \frac{BD}{2} + \lambda_{LU} S_a S_{\theta_j} S_{\alpha_j} \frac{BD}{2} \\ \sigma_{2j} &= r_0 S_{\theta_j} + S_{\theta_j} C_a \frac{BD}{2} - \lambda_{LU} S_a C_{\theta_j} S_{\alpha_j} \frac{BD}{2} \\ \sigma_{3j} &= r_0 t g a \theta_j + \lambda_{LU} C_{\theta_j} S_{\alpha_j} \frac{BD}{2} \end{aligned} \quad (3)$$

where r_0 is called the radius; S_{α_j} and C_{α_j} are simplified expressions of $\cos \alpha_j$ and $\sin \alpha_j$, respectively; λ_{LU} is the judgment coefficient of the contact state, when the ball contacts the upper side of the screw raceway, at this time $\lambda_{LU} = 1$, when the ball contacts the lower side of the screw raceway, then $\lambda_{LU} = -1$.

From this, the normal contact load between the ball and the screw raceway can be obtained as:

$$\begin{aligned} Q_j &= \lambda_j k_{coe} \delta_j^{3/2} \\ &= \lambda_j k_{coe} \left(\sqrt{(BD \cos \alpha_p + \delta_{y''j})^2 + (BD \sin \alpha_p + \delta_{z''j})^2} - BD \right)^{3/2} \end{aligned} \quad (4)$$

where δ is the normal contact deformation between the first ball and the raceway; λ_j is the normal contact deformation judgment factor between the ball and the raceway, when $\delta \leq 0$, λ is 0, when $\delta > 0$, λ is 1; k_{coe} is the contact load deformation coefficient between the ball and the raceway.

Accordingly, based on the calculation formula that the screw raceway is subjected to the normal contact force of Q_j the

first ball in the normal plane, considering the normal contact force between all the balls and the raceway on the screw raceway, the deformation of the ball screw under load can be obtained by solving the static equilibrium equations of the raceway. Substituting into Eqs. (1) and (4), the contact angle and normal contact force between the ball and the raceway at different ball phase angles can be obtained, and the deformation δ and load F in the corresponding direction of the screw raceway will be obtained. Substitute Eq. (5) to solve the static contact stiffness of the ball screw.

$$\mathbf{K} = \frac{\partial F}{\partial \delta} \quad (5)$$

3. Experimental verifications

To verify the validity of the ball screw contact characteristic analysis model, the ball screw axial static stiffness measurement platform is shown in Fig. 4. It should be noted that the experimental measurement value is the overall deformation of the ball screw, which not only includes the contact deformation between the ball and the raceway, which is directly related to the contact stiffness studied in this paper but also includes the deformation of the screw and the nut. The overall stiffness of the bar instead of the contact stiffness value is used to indirectly verify the reliability of the model. The end block circulating double nut preloaded ball screw is selected as the specific research object, and its specific model and parameters are shown in Table 1. The preload load is calculated according to the empirical formula recommended in the product catalog.

The ball screw axial static stiffness measurement platform adopts the installation method of the ball screw with one end fixed and the other floating. Through the three-tier rod type force transmission fixture, it is ensured that the tensile force exerted by the universal testing machine (model CMT5305) is only transmitted in the axial direction, as shown in Fig. 4(a). And the linear displacement sensor (model DGC-8ZG/D) is used to measure the axial contact deformation of the nut under the action of this axial load, as shown in Fig. 4(b). The three tie

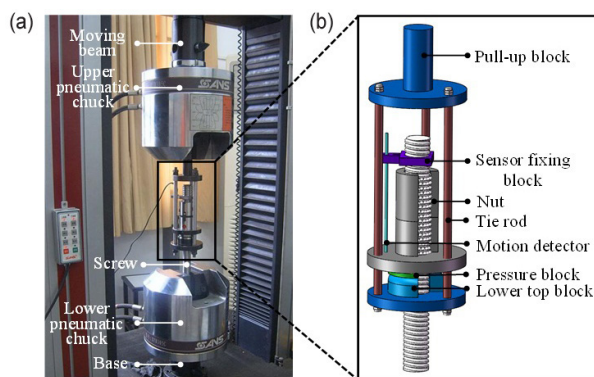


Fig. 4. Principle and platform for measuring static stiffness of ball screw in axial direction.

rods in the three tie rod type force transmission fixture pass through the nut to prevent the nut from rotating, and its two ends are respectively connected with the upper pull block and the lower pressure block, this structure can effectively ensure that the nut is only subjected to axial load. In addition, the displacement sensor is fixed by the sensor fixing block so that it is perpendicular to the end face of the nut raceway flange, to ensure the reliability of the measurement data.

Fig. 5 shows the comparison between the theoretically calculated axial static stiffness value and the experimentally measured axial static stiffness value. And the theoretical calculation value of the model without considering the non-uniform load distribution and the theoretical calculation value of the model considering the non-uniform load distribution are compared and analyzed. The theoretical calculations without considering the non-uniform load distribution model assume that all balls are subjected to the same force. It can be seen from Fig. 5 that the axial load increases from 2.5×10^4 N to 5.5×10^4 N, and the theoretically calculated values considering the non-uniform load distribution model are all closer to the experimentally measured values.

The theoretical calculation values of the model without considering the non-uniform load distribution are all large, that is, the axial contact deformation calculated based on this model is small. When the axial load is 4.0×10^4 N, the error between the theoretical calculation value and the experimental measurement value considering the non-uniform load distribution model

Table 1. Main parameters of FFZD3206-5 ball screw.

| | |
|----------------------------------|-------|
| Screw pitch circle diameter (mm) | 32 |
| Lead (mm) | 6 |
| Ball diameter (mm) | 3.969 |
| Curvature ratio of raceway | 0.54 |
| Number of balls per nut | 62 |
| Number of turns of a single nut | 2.5 |
| Preload (N) | 1665 |

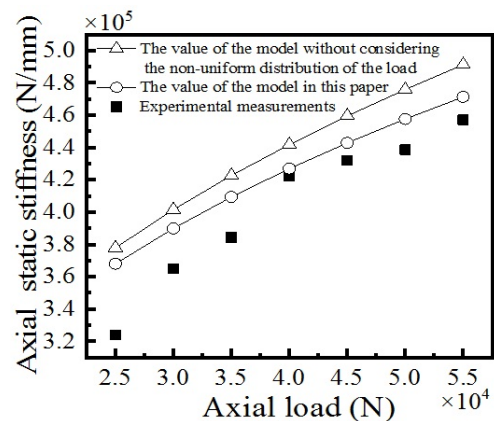


Fig. 5. Comparison between the theoretically calculated axial static stiffness and the experimental measurement.

is the smallest, which is only 1.2 %, and the error between the theoretical calculation value and the experimental measurement value under other axial load values is at most 10 %.

4. Discussion

It mainly discusses the influence of the combined action of the axial load and the overturning moment on the average value and distribution fluctuation value of the contact angle of the ball screw, the number of unloaded balls, the distribution fluctuation value of the contact load, and the static contact stiffness and other contact parameters. The degree of distribution fluctuation of the contact angle and the contact load is evaluated by the relative standard deviation value, that is, the distribution fluctuation value described in this paper.

4.1 The contact angle

The contact angle mainly affects the coordination relationship between the deformation of the raceway and the normal contact deformation of the ball at different phase angles. When the screw is the object of analysis and the direction shown in Fig. 1 is the positive z-axis axial load, as the axial load increases from 0 N to 7000 N: Because the direction of the axial load on the straight nut is opposite to the direction of the preload load, the load on the ball will first become smaller and then larger. Because the direction of the axial load on the flange nut is consistent with the direction of the preload load, the load on the ball will gradually increase. Under the action of this axial load, the effect of the overturning moment that increases from 0 N·m to 7000 N·m is also considered. Figs. 6-8 are the phase angles of all balls under the combined action of the axial load and the overturning moment, respectively. The variation of the average value of the contact angle, the fluctuation of the distribution of the contact angle at different ball phase angles, and the distribution of the contact angle at different ball phase angles.

In the straight nut, when the load on the balls first becomes smaller and then becomes larger, it can be seen from Fig. 6(a) that the average value of the contact angles at the phase angles of all the balls will basically increase first and then de-

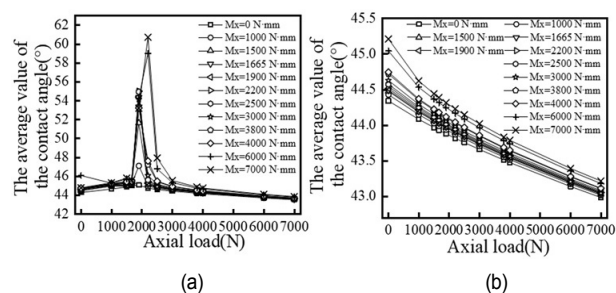


Fig. 6. The variation of average contact angles at all ball phase angles under different axial load and overturning moment: (a) straight nut; (b) flanged nut.

crease. That is, when the acting value of the overturning moment remains unchanged, the average value of the contact angle at the phase angle of all the balls will decrease as the axial load increases. However, when the nut is subjected to the load in the axial direction and remains unchanged at the critical value and above, the effect of the overturning moment on the average value of the contact angle at all ball phase angles can be followed regularly. It can be seen from Fig. 6(a) that only when the axial load applied to the straight nut is 2200 N and above, minus the preload load value, that is, the load applied in the axial direction is about 535 N and above and remains constant. The average value of the contact angles at all ball phase angles increases with the overturning moment, and the maximum value is 60.69° ($F_a = 2200$ N and $M_x = 7000$ N·m). The critical value of the axial load is about 535 N. At the same time, with the gradual increase of the acting value of the axial load, the difference between the average values of the contact angles at the phase angles of all the balls under different overturning moments gradually decreases. When the nut is subjected to a load in the axial direction within the critical value and remains unchanged, the effect of the overturning moment on the average change of the contact angle at all ball phase angles is more complicated. The main reason may be caused by the change of the contact state: The direction of the axial load on the nut is opposite to the direction of the preload. When the value of the axial load is close to the value of the preload, the contact state between the ball and the raceway is in a critical state of change.

By observing Fig. 7(a), the coupling effect of axial load and overturning moment on the fluctuation degree of the contact angle distribution at different ball phase angles, when the nut is subjected to a load of about 535 N or more in the axial direction and remains unchanged, the distribution fluctuation value of the contact angle at different ball phase angles will increase with the increase of the overturning moment. When the overturning moment remains unchanged, the distribution fluctuation value of the contact angle at different ball phase angles will become smaller as the axial load increases, and the maximum contact angle distribution fluctuation value appears when $F_a = 2200$ N and $M_x = 7000$ N·m, its value is 29.45 %. At the same time, with the gradual increase of the axial load action value,

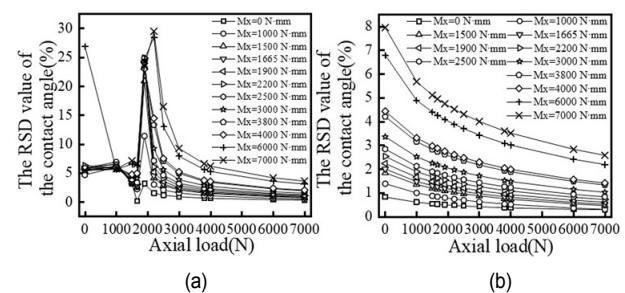


Fig. 7. The variation of the RSD value of the contact angle at different ball phase angles under different axial load and overturning moment: (a) straight nut; (b) flanged nut.

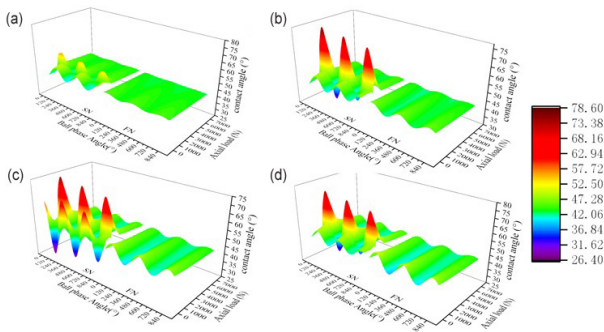


Fig. 8. The 3D diagram of the contact angel at different ball phase angles under different axial load and overturning moment: (a) with an overturning moment of 1000 N*mm; (b) with an overturning moment of 3000 N*mm; (c) with an overturning moment of 6000 N*mm; (d) with an overturning moment of 7000 N*mm.

the difference between the distribution fluctuation values of the contact angle at different ball phase angles under the action of different overturning moment action values gradually decreases, this phenomenon can also be observed by the distribution of contact angles at different ball phase angles shown in Fig. 8. In addition, it can be observed from Fig. 8 that there is a set of sensitive working condition parameters, that is, when there is only a preload load ($F_a = 0$ N) and $M_x = 6000$ N·m, the contact angle values and distribution fluctuations at different ball phase angles are large, resulting in a large average contact angle at all ball phase angles and the distribution fluctuation values of contact angles at different ball phase angles.

In the flange nut, by observing Figs. 6(b) and 7(b), the contact state of the flange nut remains unchanged because the direction of the axial load is consistent with the direction of the preload. When the acting value of the overturning moment remains unchanged, the average value of the contact angle at all ball phase angles and the distribution fluctuation value of the contact angle at different ball phase angles will become smaller as the axial load increases. When the acting value of the axial load remains unchanged, the average value of the contact angle at all ball phase angles and the distribution fluctuation value of the contact angle at different ball phase angles will increase with the increase of the overturning moment. At the same time, with the gradual increase of the acting value of the axial load, under the action of different overturning moment values, the difference between the average value of the contact angle at all the ball phase angles and the distribution fluctuation value of the contact angle at different ball phase angles gradually decreases. This phenomenon can also be observed from the distribution of contact angles at different ball phase angles shown in Fig. 7.

4.2 The contact load

In a straight nut, the load on the balls will first become smaller and then larger, so the number of unloaded balls will first increase and then decrease accordingly. By observing Fig. 9(a), when the action value of the axial load is close to the action

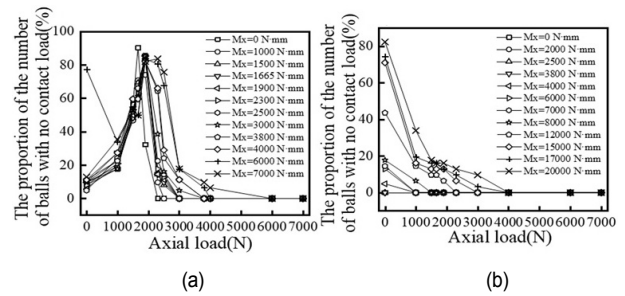


Fig. 9. The variation of the proportion of the number of balls with no contact load under different axial load and overturning moment: (a) straight nut; (b) flanged nut.

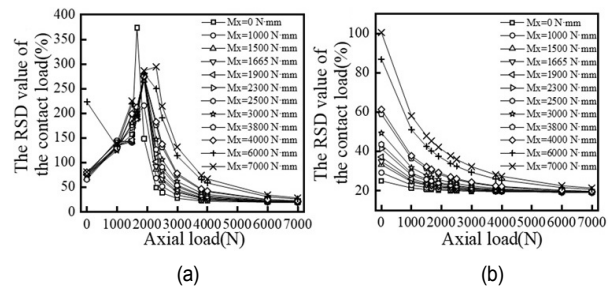


Fig. 10. The variation of the RSD value of the contact load at different ball phase angles under different axial load and overturning moment: (a) straight nut; (b) flanged nut.

value of the preload load, the number of unloaded balls is large. When the action value of the axial load is equal to the action value of the preload load ($F_a = 1665$ N) and there is no overturning moment ($M_x = 0$ N·m), the number of unloaded balls is the largest, accounting for about 90.32%. When the value of the overturning moment remains constant, the number of unloaded balls decreases as the axial load increases. However, by analyzing the influence of the combined effect of the axial load and the overturning moment on the contact angle between the ball and the raceway affected by the contact state between the ball and the raceway, only when the load on the nut in the axial direction remains constant at the critical value and above, the number of unloaded balls will change regularly with the change in the value of the overturning moment. It can be observed from Fig. 9(a) that when the straight nut is subjected to an axial load of more than 2300 N, that is, when the load in the axial direction is about 635 N and above and remains unchanged, the number of unloaded balls will increase with the increase of the overturning moment, which is consistent with the relevant existing research results [6]. However, by examining the overturning moment within 20 KN·mm, it can be seen that when the axial load reaches 6000 N, it will no longer be affected by the overturning moment, and there will be no unloaded balls.

By observing Fig. 10(a), the coupling effect of the axial load and the overturning moment on the fluctuation degree of the contact load distribution at different ball phase angles. Similarly, when the nut is subjected to a load of about 635 N or more in the axial direction and remains unchanged, the distribution

fluctuation value of the contact load at different ball phase angles will increase with the increase of the overturning moment. When the overturning moment remains unchanged, the distribution fluctuation value of the contact load at different ball phase angles will become smaller as the axial load action value increases. The most serious fluctuation of the contact load distribution occurs when the action value of the axial load is equal to the action value of the preload load ($F_a = 1665 \text{ N}$) and when there is no overturning moment ($M_x = 0 \text{ N}\cdot\text{m}$), its value is 373.60%. At the same time, with the gradual increase of the axial load action value, the difference between the distribution fluctuation values of the contact load at different ball phase angles under the action of different overturning moment action values gradually decreases. This phenomenon can also be observed by the distribution of the contact load at different ball phase angles shown in Fig. 11. In addition, it can be observed from Fig. 11 that there is a set of sensitive working condition parameters, that is when there is only a preload load ($F_a = 0 \text{ N}$) and $M_x = 6000 \text{ N}\cdot\text{m}$, the contact load values and distribution fluctuations at different ball phase angles are larger. As a result, the average value of the contact loads at all ball phase angles and the distribution fluctuations of the contact loads at different ball phase angles are large.

In the flange nut, the overturning moment is within $20 \text{ KN}\cdot\text{m}$, as the applied value of the axial load increases, the applied value of the overturning moment also needs to increase to cause unloaded balls to appear. It can be observed from Fig. 9(b) that: When $F_a = 1000 \text{ N}$, when $M_x = 8000 \text{ N}\cdot\text{m}$, unloaded balls appear; When $F_a = 3000 \text{ N}$, when $M_x = 17 \text{ KN}\cdot\text{m}$, the unloaded balls will appear; when $F_a = 4000 \text{ N}$, no unloaded balls will appear when the overturning moment is within $20 \text{ KN}\cdot\text{m}$. When the value of the overturning moment remains constant, the number of unloaded balls gradually decreases to zero as the axial load increases. By observing Fig. 10(b), the contact state of the flange nut remains unchanged because the direction of the axial load is the same as that of the preload. When the acting value of the overturning moment remains unchanged, the distribution fluctuation value of the contact load

at different ball phase angles will become smaller as the axial load increases. When the acting value of the axial load remains unchanged, the distribution fluctuation value of the contact load at different ball phase angles will increase with the increase of the overturning moment. At the same time, with the gradual increase of the acting value of the axial load, the difference between the distribution fluctuation values of the contact load at different ball phase angles gradually decreases. This phenomenon can also be observed by the distribution of the contact load at different ball phase angles shown in Fig. 11.

4.3 The static contact stiffness

Figs. 12 and 13 show the changes in the static contact stiffness in the axial direction and the static contact stiffness in the overturning direction under the combined action of the axial load and the overturning moment, respectively. It can be seen from the above analysis that the change of the contact state between the ball and the raceway is one of the main factors affecting the contact angle and contact load due to the combined effect of the axial load and overturning moment. However, the influence of the change of the contact state is not only at the point where $F_a = 1665 \text{ N}$, which is the same as the action value of the preload load, but within a certain range around this action value. It can be observed from Fig. 12(a) that when the nut is subjected to an axial load above 2500 N , that is, when the load value in the axial direction is about 835 N and above remains unchanged, the axial static connection stiffness

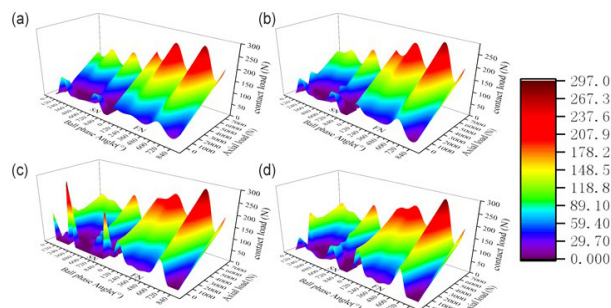


Fig. 11. The 3D diagram of the contact load at different ball phase angles under different axial load and overturning moment: (a) with an overturning moment of $1000 \text{ N}\cdot\text{m}$; (b) with an overturning moment of $3000 \text{ N}\cdot\text{m}$; (c) with an overturning moment of $6000 \text{ N}\cdot\text{m}$; (d) with an overturning moment of $7000 \text{ N}\cdot\text{m}$.

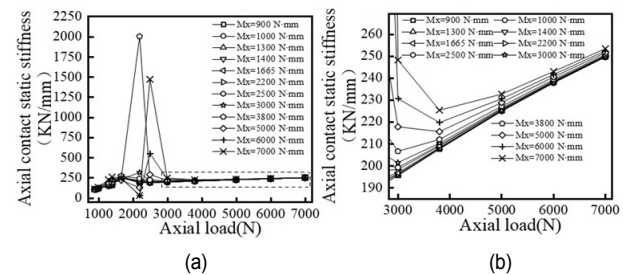


Fig. 12. The variation of the axial contact static stiffness: (a) at different ball phase angles under different axial load and overturning moment; (b) enlarged view of the Fig. 12(a).

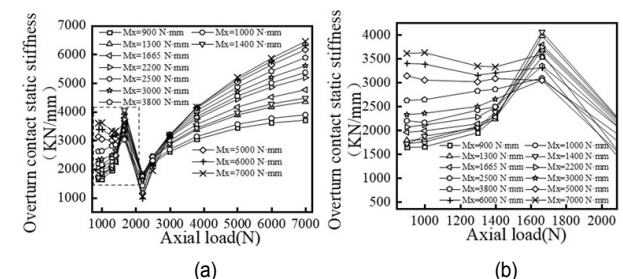


Fig. 13. The variation of the overturn contact static stiffness: (a) at different ball phase angles under different axial load and overturning moment; (b) enlarged view of the Fig. 13(a).

will show regular changes with the change of the overturning moment value. It can be observed from the partially enlarged view of Fig. 12(a) in Fig. 12(b) that the value of the axial static connection stiffness increases with the increase of the overturning moment. However, the difference between the axial static contact stiffness values under the action of different overturning moments will gradually decrease with the increase of the axial load. At the same time, when the nut is subjected to a load of about 835 N in the axial direction and above, and the overturning moment remains unchanged, the axial static connection stiffness increases with the increase of the axial load. In addition, through Fig. 12(a), it can be observed that there are two sets of sensitive working condition parameters, namely when $F_a = 2200$ N and $M_x = 3800$ N·m and when $F_a = 2500$ N and $M_x = 7000$ N·m, the static contact stiffness values of these two places are larger. This may be mainly due to the smaller number of unloaded balls in these two operating conditions, resulting in smaller contact deformation at this time.

By observing Fig. 13(a), it can be seen that when the nut is subjected to an axial load of more than 3800 N, that is, when the load in the axial direction is about 2135 N and above and remains unchanged, the static contact stiffness value in the overturning direction will increase with the increase of the overturning moment, the difference between the static contact stiffness values in the overturning direction under the action of different overturning moment values will gradually increase with the increase of the axial load. It is observed through the partially enlarged view of Fig. 13(a) in Fig. 13(b), that when the nut is subjected to an axial load within 900 N to 1300 N when the action value of the axial load remains unchanged, the value of the static contact stiffness in the overturning direction will increase with the increase of the overturning moment. When the nut is subjected to a load of about 2135 N and above in the axial direction, and the overturning moment remains unchanged, the static contact stiffness value in the overturning direction increases with the increase of the axial load.

5. Conclusions

Contact parameters such as the average value and distribution fluctuation value of the contact angle of the ball screw, the number of unloaded balls and the distribution fluctuation value of the contact load, and the static contact stiffness are mainly affected by the axial load. With the increase of the axial load, the average value and distribution fluctuation value of the overturning moment on the contact angle of the ball screw will be reduced, and it is not affected by the number of loaded balls, the distribution fluctuation value of the contact load, and the axial static contact stiffness. Taking the FFZD3206-5 type ball screw as an example, we can see that the overturning moment is within 20 KN·mm, when the axial load reaches 6000 N, it will no longer be affected by the overturning moment, and there will be no unloaded balls. However, the effect of the overturning moment on the static contact stiffness in the overturning direction does not decrease with the increase of the axial load.

When the acting direction of the preload load on the nut is opposite to the acting direction of the axial load, the change of the contact state between the ball and the raceway caused by the combined action of the axial load and the preload load will affect the change law of the contact parameters. The influence of the change of the contact state does not only exist in the place where the action value of the axial load and the preload load is equal, but in a certain range around this action value, within this range, there is a critical value of the load in the axial direction. Only when the load on the nut in the axial direction is above the critical value, the contact parameters change regularly with the changes of the axial load and the overturning moment. However, the critical values for different contact parameters to show regular changes with the changes of axial load and overturning moment are different.

When the acting direction of the preload load on the nut is opposite to the acting direction of the axial load, only when the load acting on the nut in the axial direction is at or above the critical value of each contact parameter, the static contact stiffness in the axial and overturning directions is proportional to the axial load and overturning moment. In addition, other contact parameters are proportional to the axial load and inversely proportional to the overturning moment. When the acting direction of the preload load on the nut is the same as that of the axial load, the relationship between the contact parameters, the axial load, and the overturning moment is the same as above. Under the action of different overturning moment values, except that the static contact stiffness value increases with the increase of the axial load, other contact parameters gradually decrease with the increase of the axial load.

Acknowledgments

This work was supported by Research Program supported by the Department of China Postdoctoral Science Foundation (Postdoctoral Science Foundation Project), China.

Nomenclature

| | |
|------------|---|
| α_p | : Contact angle between ball and raceway after preload |
| δ | : Contact deformation between ball and raceway |
| a | : Contact angle between ball and raceway contact surface |
| A | : Distance between the center of curvature of the screw raceway and nut raceway after deformation |
| θ | : Ball phase angle |
| α | : Helix angle |
| r_0 | : Nominal radius |
| Q | : Normal contact force between ball and raceway contact surface |
| F | : External load |
| K | : Static contact stiffness |

References

- [1] Y. Altintas, A. Verl, C. Brecher, L. Uriarte and G. Pritschow,

- Machine tool feed drives, *CIRP Annals - Manufacturing Technology*, 60 (2011) 779-796.
- [2] N. Zhen and Q. An, Analysis of stress and fatigue life of ball screw with considering the dimension errors of balls, *International Journal of Mechanical Sciences*, 137 (2018) 68-76.
- [3] O. E. Chinedum, Improved screw-nut interface model for high-performance ball screw drives, *Journal of Mechanical Design*, 133 (2011) 041009.
- [4] H. X. Zhou, C. G. Zhou, H. T. Feng and Y. Ou, Theoretical and experimental analysis of the preload degradation of double-nut ball screws, *Precision Engineering*, 65 (2020).
- [5] Y. Chen, C. Zhao, S. Zhang and X. Meng, Analysis on load distribution and contact stiffness of single-nut ball screw based on the whole rolling elements model, *Transactions-Canadian Society for Mechanical Engineering*, 43 (3) (2019).
- [6] X. Jingyao, Z. Changguang, F. Hutian and Z. Luchao, Load distribution of double nut ball screws with consideration of geometric errors and overturning moment, *China Mechanical Engineering*, 32 (2021) 1181-1190.
- [7] J. Zhao, M. Lin, X. Song and W. Nan, Coupling analysis of the fatigue life and the TEHL contact behavior of ball screw under the multidirectional load, *Industrial Lubrication and Tribology* (2020) (ahead-of-print).
- [8] R. Bertolaso, M. Cheikh, Y. Barranger, J.-C. Dupré, A. Germaneau and P. Doumalin, Experimental and numerical study of the load distribution in a ball-screw system, *Journal of Mechanical Science and Technology*, 28 (2014) 1411-1420.
- [9] B. Lin, C. E. Okwudire and J. S. Wou, Low order static load distribution model for ball screw mechanisms including effects of lateral deformation and geometric errors, *Journal of Mechanical Design*, 140 (2) (2017).
- [10] L. Sangalli, A. Oyanguren, J. Larraaga, A. Arana, M. Izquierdo and I. Ulacia, Numerical characterization of local and global non-uniformities in the load distribution in ball screws, *The International Journal of Advanced Manufacturing Technology*, 118 (2022) 1411-1425.
- [11] J. Zhao, M. Lin, X. Song and Q. Guo, Investigation of load distribution and deformations for ball screws with the effects of turning torque and geometric errors, *Mechanism and Machine Theory*, 141 (2019) 95-116.
- [12] C. Liu, C. Zhao, X. Meng and B. Wen, Static load distribution analysis of ball screws with nut position variation, *Mechanism and Machine Theory*, 151 (2020) 103893.
- [13] Y. J. Chen, W. C. Tang and J. L. Wang, Influence factors on stiffness of a ball screw, *Journal of Vibration and Shock* (2013).
- [14] J. Liu, H. Feng and C. Zhou, Static load distribution and axial static contact stiffness of a preloaded double-nut ball screw considering geometric errors, *Mechanism and Machine Theory*, 167 (2022).
- [15] Y. J. Chen and W. C. Tang, Determination of contact stiffness in ball screws considering variable contact angles, *Proceedings of the Institution of Mechanical Engineers, Part C. Journal of Mechanical Engineering Science*, 228 (2014) 2193-2203.



Yongjiang Chen is a post doctor of the Hefei Institute of Physical Science, Chinese Academy of Sciences, Hefei, China. He received his Ph.D. in Mechanical Engineering from Southeast University. His research interests include Mechanical Statics and Dynamics Analysis, performance parameter measurement and

processing.